Electronic Supplementary Material (ESI) for Journal of Materials Chemistry C.

Electronic Supplementary Information

Highly luminescent NIR-emitting $CuFeS_2$/ZnS core/shell quantum dots for optical imaging of inflamed tissue†

Tong Yan,‡[a] Yunyan Li,‡[a] Xiaoxiao Song,[a] Jie Wang,[a] Zhuoying Xie,[b]* and Dawei Deng[a]*

[a] Department of Biomedical Engineering, and Department of Pharmaceutical Engineering, School of Engineering, China Pharmaceutical University, Nanjing 211198, China
[b] State Key Laboratory of Bioelectronics, Southeast University, Nanjing 210096, China

‡ T. Y. and Y. Y. L. contributed equally to this work.

* Corresponding Authors
E-mail: dengdawei@cpu.edu.cn (D. Deng)
E-mail: zyxie@seu.edu.cn (Z. Xie).

ORCID
Dawei Deng: 0000-0002-1391-1845
Zhuoying Xie: 0000-0003-3534-1924

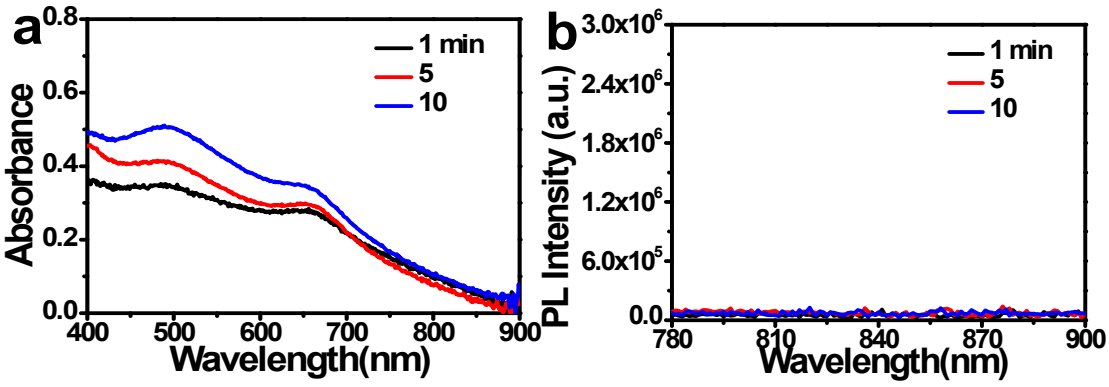

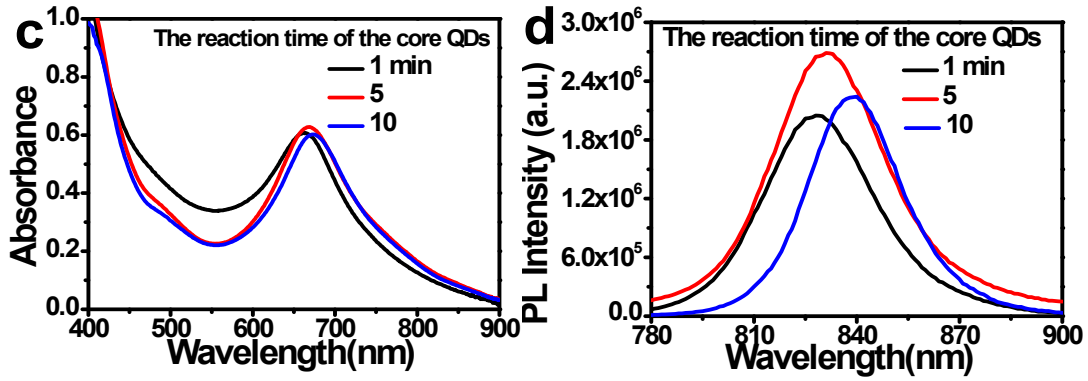

Fig. S1 (a) UV–vis absorption and (b) PL spectra of $CuFeS_2$ core QDs taken at various reaction time at 180 ºC. (c) UV–vis absorption and (d) PL spectra of $CuFeS_2$/ZnS core/shell QDs by using the core QDs with different reaction time at 180 ºC.

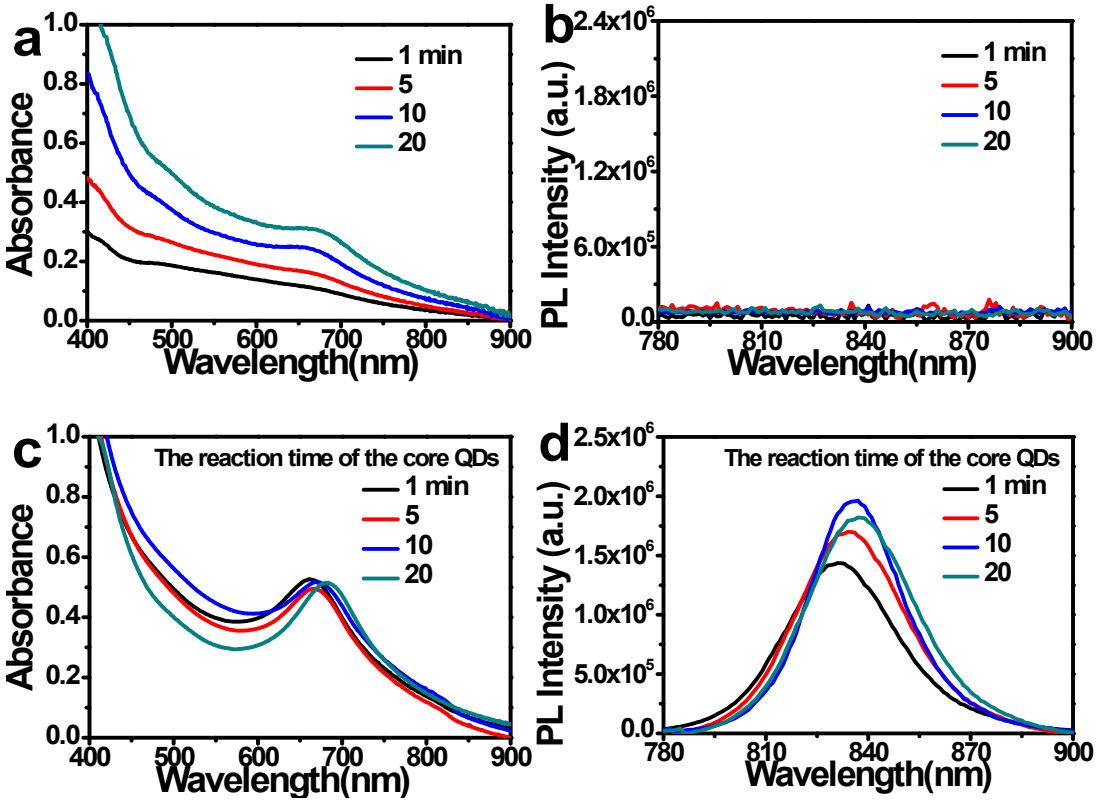

Fig. S2 (a) UV–vis absorption and (b) PL spectra of $CuFeS_2$ core QDs taken at various reaction time at 160 ºC. (c) UV–vis absorption and (d) PL spectra of $CuFeS_2$/ZnS core/shell QDs of

different $CuFeS_2$ core QDs reaction time at 160 ºC.

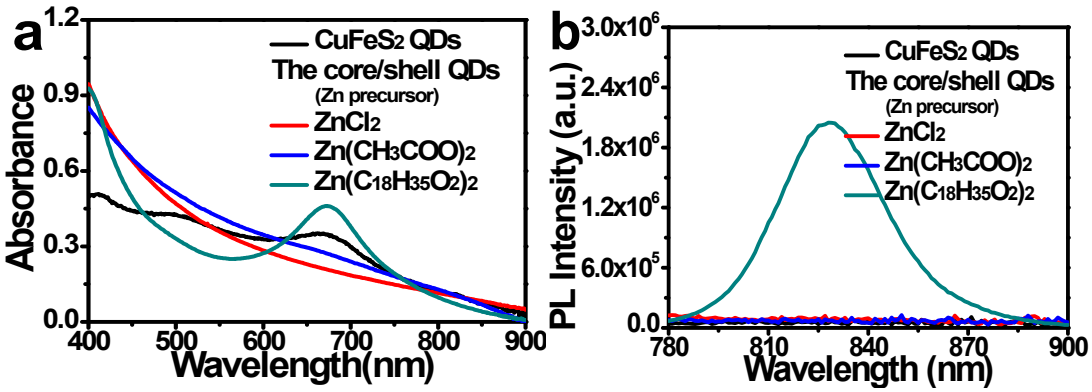

Fig. S3 (a) UV-vis absorption and (b) PL spectra of $CuFeS_2$/ZnS core/shell QDs obtained with different zinc sources.

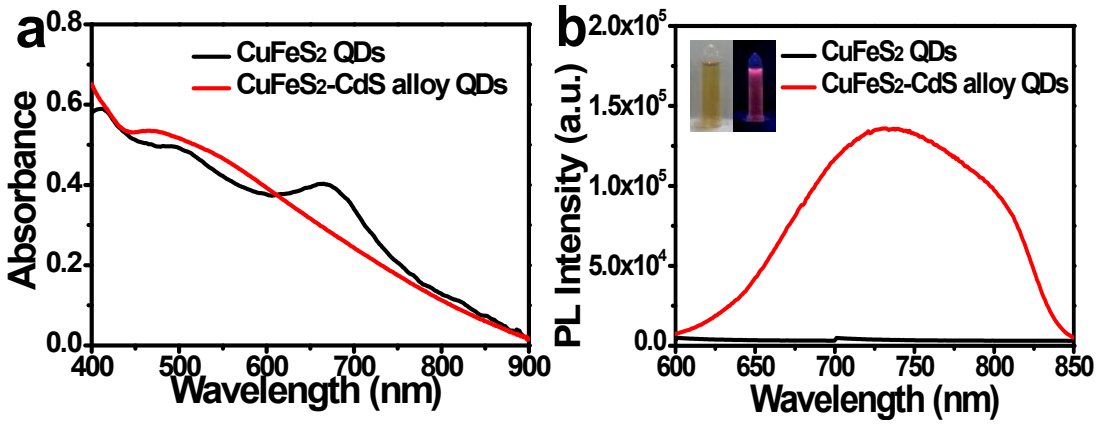

Fig. S4 UV-vis absorption (a) and PL spectra (b) of $CuFeS_2$ and $CuFeS_2$-CdS alloy QDs.

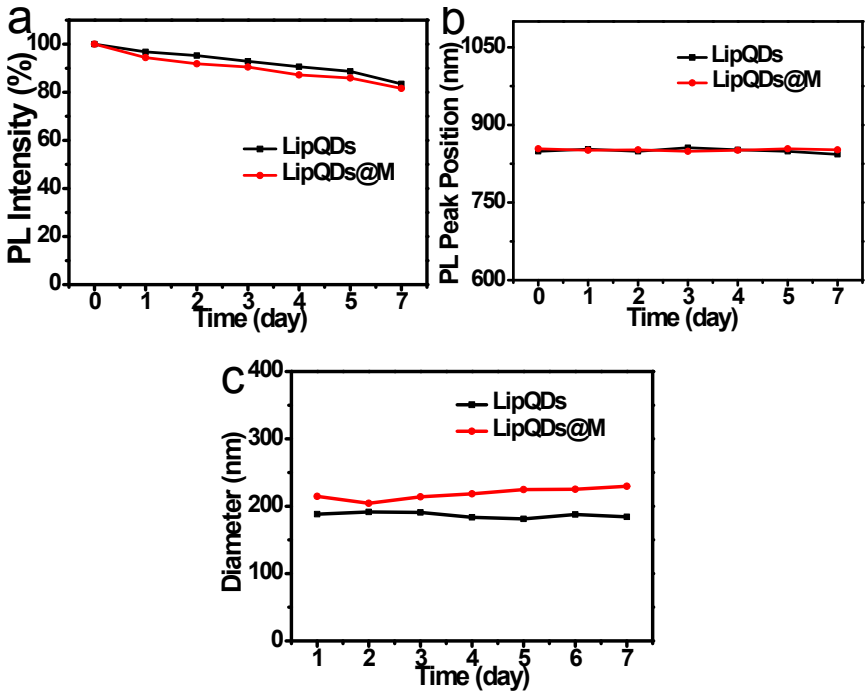

Fig. S5 Storage-stability of the LipQDs and LipQDs@M: the evolutions of (a) PL intensity, (b) PL peak position and (c) hydrodynamic diameter with time.

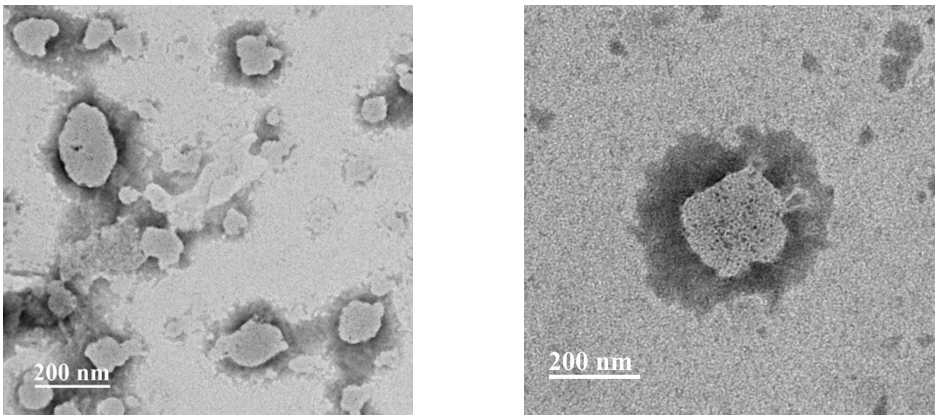

Fig. S6 TEM images of LipQDs@Membrane nanocomposites after counterstaining

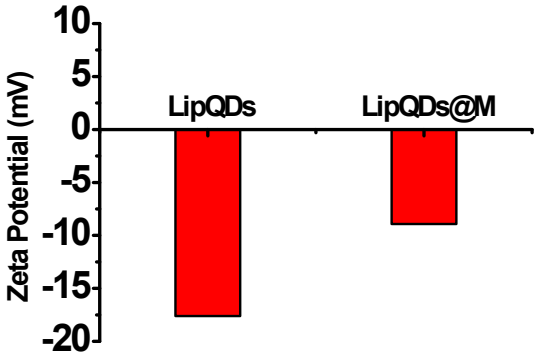

Fig. S7 The surface Zeta potential of LipQDs and LipQDs@M in water.

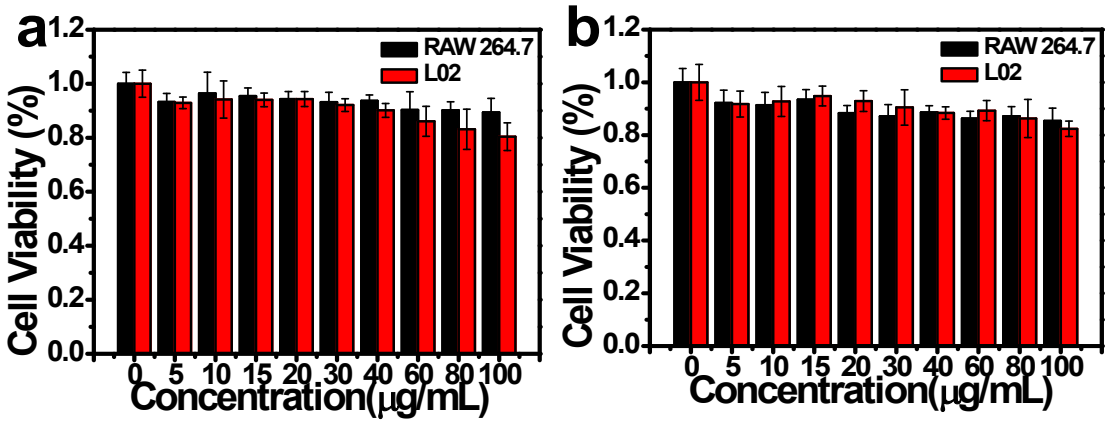

Fig. S8 The cytotoxicities of LipQDs (a) and LipQDs@M (b) by MTT assay for 24 h incubation.

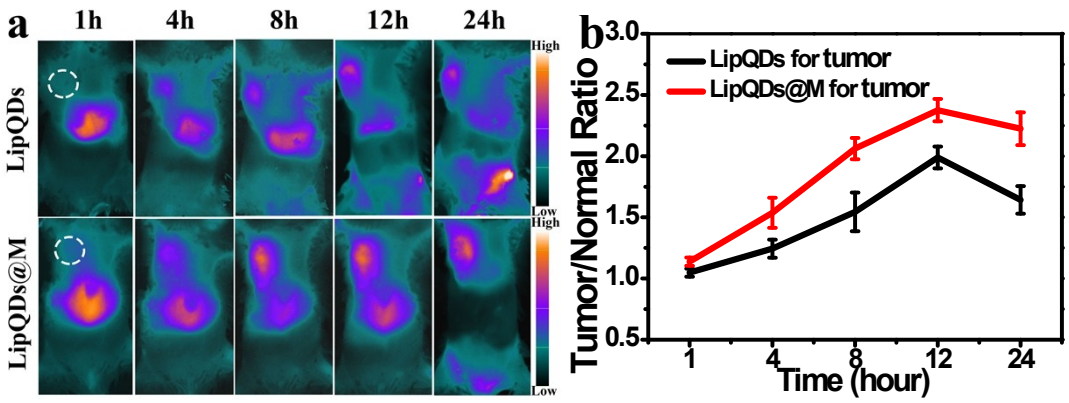

Fig. S9 (a) Dynamic distributions of LipQDs and LipQDs@M nanocomposites in the tumor model mice, where the tumor site was marked by a white circle. (b) The corresponding evolutions of T/N (muscle) ratios in tumor model mice with time.

In general, the fluorescence signals were also detected at the tumor sites (the main reason is ascribed to the passive targeting effect (EPR)). The T/N ratio, at the same time, was significantly lower than that of postoperative tumor inflamed sites mice.

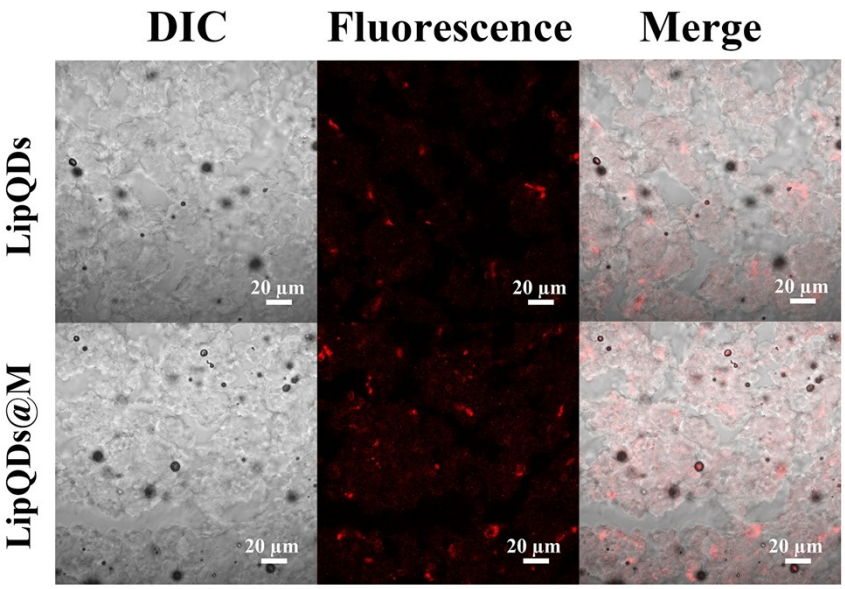

Fig. S10 Tissue section fluorescence imaging of LipQDs and LipQDs@M nanocomposites in the tumor model mice.

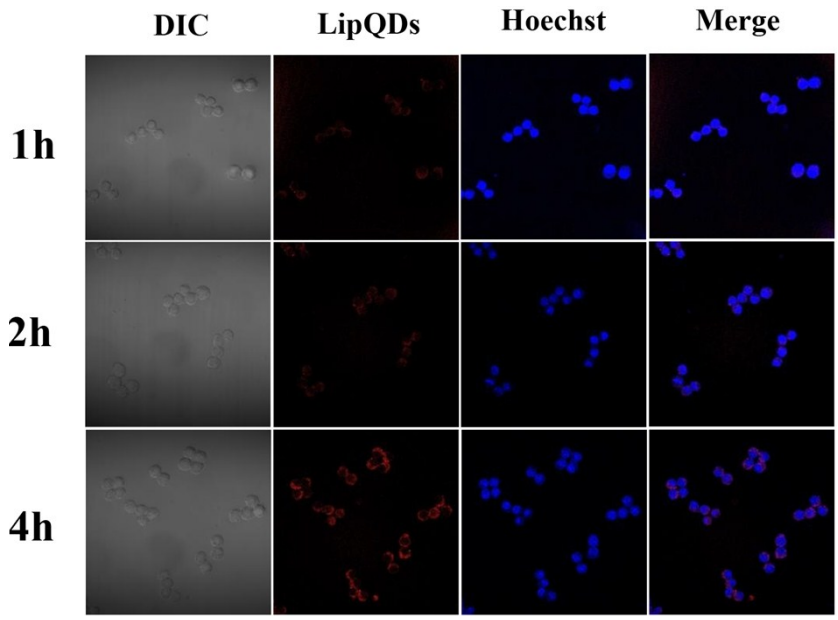

Fig. S11 LCSM images of RAW 264.7 cells incubated with LipQDs for 1, 2 and 4 h.